



**HAL**  
open science

## Photoinitiating Ability of Pyrene–Chalcone-Based Oxime Esters with Different Substituents

Xiaoxiang Zhang, Zheng Liu, Di Zhu, Xiaotong Peng, Didier Gigmes, Michael Schmitt, Pu Xiao, Frédéric Dumur, Jacques Lalevée

► **To cite this version:**

Xiaoxiang Zhang, Zheng Liu, Di Zhu, Xiaotong Peng, Didier Gigmes, et al.. Photoinitiating Ability of Pyrene–Chalcone-Based Oxime Esters with Different Substituents. *Macromolecular Chemistry and Physics*, 2023, 224 (20), 10.1002/macp.202300293 . hal-04280841

**HAL Id: hal-04280841**

**<https://hal.science/hal-04280841>**

Submitted on 11 Nov 2023

**HAL** is a multi-disciplinary open access archive for the deposit and dissemination of scientific research documents, whether they are published or not. The documents may come from teaching and research institutions in France or abroad, or from public or private research centers.

L'archive ouverte pluridisciplinaire **HAL**, est destinée au dépôt et à la diffusion de documents scientifiques de niveau recherche, publiés ou non, émanant des établissements d'enseignement et de recherche français ou étrangers, des laboratoires publics ou privés.

# Photoinitiating Ability of Pyrene-Chalcone-Based Oxime Esters with Different Substituents

Xiaoxiang Zhang<sup>1,2,3</sup>, Zheng Liu<sup>4</sup>, Di Zhu<sup>5</sup>, Xiaotong Peng<sup>2</sup>, Didier Gigmes<sup>4</sup>, Michael Schmidt<sup>2</sup>, Pu Xiao<sup>5\*</sup>, Frédéric Dumur<sup>4</sup>, Jacques Lalevée<sup>2,3\*</sup>

<sup>1</sup> Zhongyuan University of Technology School of Textiles, Zhengzhou 450007, China

<sup>2</sup> Université de Haute-Alsace, CNRS, IS2M UMR 7361, F-68100 Mulhouse, France

<sup>3</sup> Université de Strasbourg, France

<sup>4</sup> Aix Marseille Univ, CNRS, ICR, UMR 7273, F-13397 Marseille, France

<sup>5</sup> Research School of Chemistry, Australian National University, Canberra, ACT 2601, Australia

\* Correspondence: pu.xiao@anu.edu.au; [Frederic.dumur@univ-amu.fr](mailto:Frederic.dumur@univ-amu.fr); [jacques.lalevee@uha.fr](mailto:jacques.lalevee@uha.fr)

**Abstract:** With the rapid development of new irradiation setups as well as the ongoing interest for 3D printing, photopolymerization has been extensively studied during the last decades. In photopolymerization, the photoinitiator and/or photosensitizer plays a crucial role in the photoinitiation step as this structure interacts with light and thus creates the initiating species. From this viewpoint, the different groups that can be introduced onto the photoinitiator are primordial to generate initiating species and the development of monocomponent photoinitiating systems is currently the focus of numerous works. In this study, a series of 18 chalcone-based oxime esters featuring the pyrene chromophore have been designed, synthesized and studied for the photoinitiating properties upon irradiation with visible light. Precisely, their photoinitiation abilities were examined during the free radical photopolymerization (FRP) of acrylates upon irradiation at 405 nm with a LED. In

this series of oxime esters (OXEs), five of them demonstrated excellent photoinitiation performance. Their thermal initiation abilities were also examined. In order to improve their photoinitiation abilities, these Type I photoinitiators were also tested as Type II photoinitiators in two-component photoinitiating systems using *bis*-(4-*tert*-butylphenyl)iodonium hexafluorophosphate or ethyl 4-(dimethylamino)benzoate as the additives. Using this second approach, the OXE-B/Iod system showed the best photopolymerization performance. To evidence the interest of these chalcone-based oxime esters, the best OXE was used as monocomponent photoinitiator in 3D laser writing at 405 nm. The design of composites was also examined, using glass fibers and carbon fiber as fillers.

**Keywords:** Oxime esters, visible light, Photoinitiators, Chalcone, Pyrene, Type I photoinitiators

## **Introduction**

Photopolymerization constitutes an appealing polymerization technique enabling to convert a monomer as a polymer using light as the activating agent. As interesting features of photopolymerization, the polymerization process can take place very quickly and in energy saving conditions. Considering the fact that the polymerization process can be carried out without solvents, photopolymers can be obtained in greener conditions than those prepared by thermal polymerization (polymerization reactions done in organic solvents, often THF). Benefiting from these advantages, photopolymerization is used in numerous industrial, medical and academic research fields [1-4]. The PI (photoinitiator) plays a very important role in the photopolymerization as this structure is the key-element interacting with light. Subsequent to photoexcitation and by reaction with the appropriate additives, free radicals or cations can be generated, enabling to initiate the polymerization process. The free radicals can initiate the chain reaction enabling to form the polymers. If UV photopolymerization was extensively used starting from the 60s, nowadays, this approach is more and more discarded from industrial applications due to safety

concerns raised by the use of UV light (skin cancers and eye damages). Parallel to this UV irradiation setups are energy-consuming devices and this approach is nowadays inappropriate in the current context of energy sobriety plans unveiled by numerous European countries. Notably, photopolymerization can be carried out in energy saving conditions if visible light is used. Especially, the design of photoinitiating systems activable under low light intensity and notably LEDs is still a challenge.[5-10]. If multicomponent photoinitiating systems were extensively studied in the literature for decades and could furnish remarkable monomer conversions, recently, the simplification of the photocurable resins and the design of mono-component systems is more and more the focus of numerous studies.

In this field, oxime esters (OXEs) are well-recognized as being excellent Type I PIs in free radical photopolymerization and a wide range of structures have been recently proposed in the literature.[11-14] Interest for oxime esters is notably supported by the easiness of synthesis, the possibility to introduce a photocleavable group at low cost (use of hydroxylamine hydrochloride to prepare the oxime function), and the possibility to esterify the oxime with various cheap and commercially available acid chlorides. As specificities, oxime esters comprise a N-O bond that can be homolytically cleaved upon irradiation, producing acyloxy/aryloxy and iminyl radicals. Interestingly, acyloxy/aryloxy radicals can decarboxylate, producing CO<sub>2</sub> that can contribute the limit oxygen diffusion within the resin. Parallel to this, after decarboxylation, alkyl and aryl radicals thus formed cannot recombine anymore with iminyls radicals so that alkyl and aryl radicals can only contribute to monomer conversion [15]. At present, benchmark OXEs only exhibit UV-centered absorptions, drastically affecting the scope of applications [16]. Therefore, there is a significant interest to synthesize OXEs with red-shifted absorptions that could be commercialized in the Future.[17-21] However, for industrial applications, the reactivity is the key parameters and this point has still to be addressed. In order to redshift the absorption spectrum from the UV range to the visible range, different chromophores were examined for the design of OXEs in the literature and structures such as

phenothiazine, nitro-carbazole, triphenylamine, or coumarin were studied.[22,23] In the present work, a series of chalcone-based OXEs featuring the pyrene chromophore and been designed and synthesized. was selected to be added to the backbone of OXE.

Chalcones are abundant in nature, and they can be extracted from many fruits (e.g., orange, tomato, apple), vegetables (e.g., shallot, liquorice, bean sprout, and potato), and nuts [24-28]. Generally, chalcones are categorized by substituents, and their different positions on the chalcone backbone, which lead to different colors and different light absorption properties [29]. Our group reported more than 50 mono-chalcone derivatives as photoinitiators in previous works [30]. Several mono-chalcone derivatives exhibited excellent light absorptions. Furthermore, these mono-chalcone derivatives demonstrated good photoinitiation abilities in the FRP of acrylates and cationic photopolymerization [31]. In this study, 18 pyrene-chalcone oxime esters were designed and successfully synthesized ( See supporting information and Figure 1), each pyrene-chalcone is constituted of the different substituent on oxime backbone, the photoinitiation ability of substituent effects were deeply investigated.

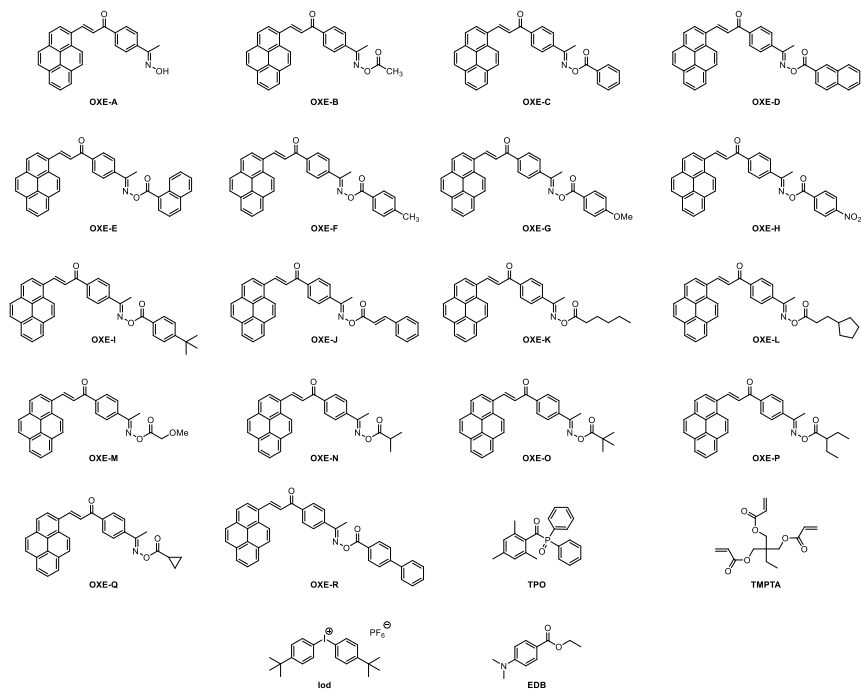


**Figure 1.** The chemical structures of the investigated OXEs, TPO, TMPTA, IOD, and the amine (EDB)

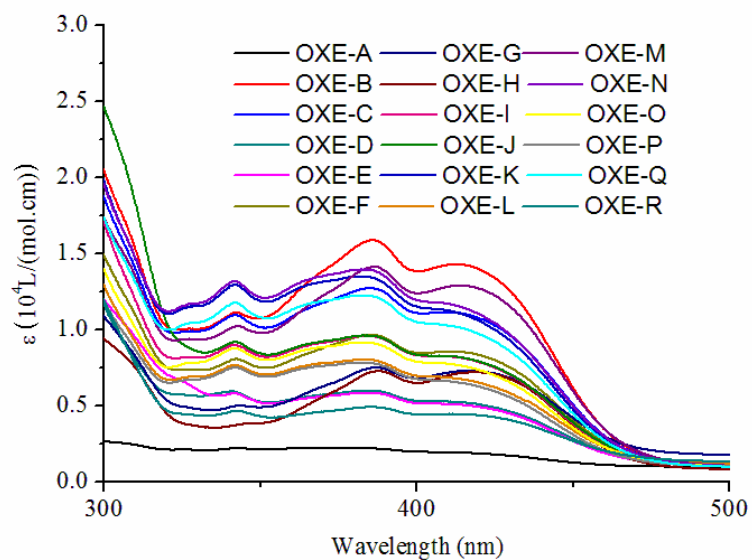


**Figure 2.** The molar extinction coefficient vs. UV–visible wavelength of the OXEs in acetonitrile ( $1 \times 10^{-4}$  mol/L)

### Results and Discussion

Most of these OXEs exhibited wide light absorption from 390 nm to 405 nm (See Figure 2), indicating that most of these OXEs were sensitive to visible light, some photoinitiation could take place when they are exposed to the visible light irradiations. However, OXE-A did not show any absorption within 300 – 500 nm.

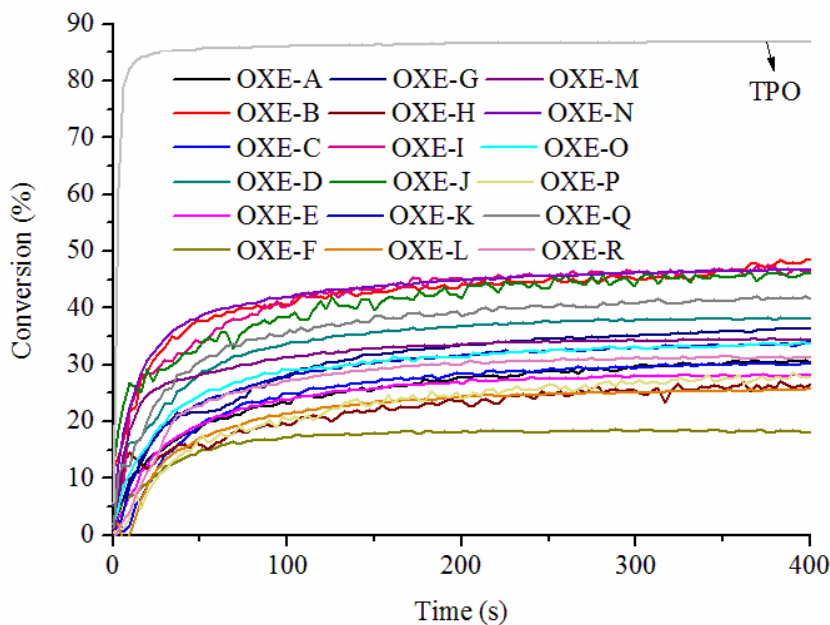


**Figure 3.** Photopolymerization properties of TMPTA obtained in laminate ( $\approx 25 \mu\text{m}$ ) OXEs and TPO based PIs ( $1 \times 10^{-5}$  mol/g) under LED@405 nm irradiation, the irradiation starts for  $t = 0$  s

The results display that OXE-B exhibited better photoinitiation capability than other OXEs upon LED@405 nm (See Figure 3). The final conversion (FC) of OXE-B reached 45%, contributing to its highest absorption ability ( $\epsilon_{\text{max}}(\text{OXE-B}) = 18000 \text{ L}/(\text{mol}\cdot\text{cm})$ ). Compared to other OXEs, without oxime-ester moiety, OXE-A has a lower photoinitiation ability, FC of OXE-A just was 25%, while OXE-N reached a relatively higher FC of 43%, which can be ascribed to a higher absorption property of OXM-N ( $\epsilon_{\text{max}}(\text{OXE-N}) = 14500 \text{ L}/(\text{mol}\cdot\text{cm})$ ). Moreover, the polymerization rates of

**Commenté [DF1]:** Why polymerization tests have not been carried out at 455 nm ? At this wavelength, there is still a good absorption.

**Commenté [DF2]:** There is no table summarizing the optical properties of the different OXEs and the molar extinction coefficient at 405 nm

these OXEs were not directly related to their absorption properties, indicating that not only absorption properties but also other factors are very important in photopolymerization such as the bond dissociation energy, the decarboxylation and generation of free radicals [32,33]. Therefore, studying the mechanism of the photoinitiation of these OXEs is very important [34], and the photolysis mechanism of pyrene-chalcone chromophore-based OXEs was in Figure 4.

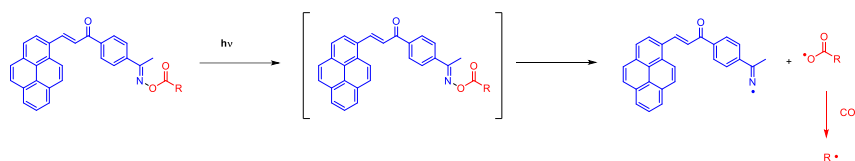


**Figure 4.** Photolysis mechanism of pyrene-chalcone chromophore-based OXEs

It is widely reported that OXEs have high quantum yields through photoinduced decarboxylation [35]. Remarkably, the decarboxylation reaction is energetically favorable in the sample of OXE-B ( $\Delta H_{\text{decarboxylation}} = E_{(R\cdot)} - E_{(RC(=O)O\cdot)} + E_{(CO_2)} = -4.94$  kcal.), and the released  $CO_2$  can be detected by Fourier transformed infrared spectroscopy (FTIR) as shown in Figure 5 [36-38].

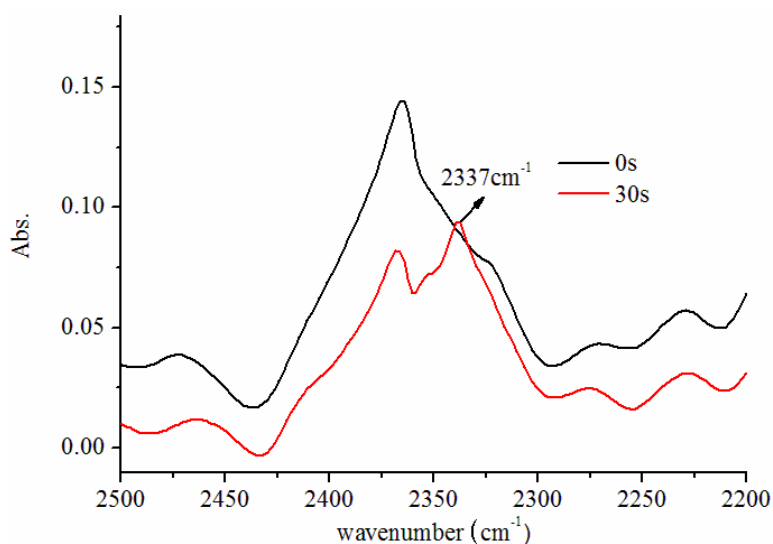


**Figure 5.** FTIR spectrum of the decarboxylation of OXE-B upon irradiation @405 nm for 30 s in TMPTA with a concentration of  $1 \times 10^{-5}$  mol/g

Generally, generated radicals ( $R\cdot$ ) can initiate a chain reaction. The efficient of generation can be evaluated by comparing the spin density of the radical center, the spin is more localized, and more able to take place reaction [39]. OXE-B has high spin density, and releases freer radicals, leading to generating methyl radicals more favorably. This explains the highest photoinitiation ability of OXE-B.

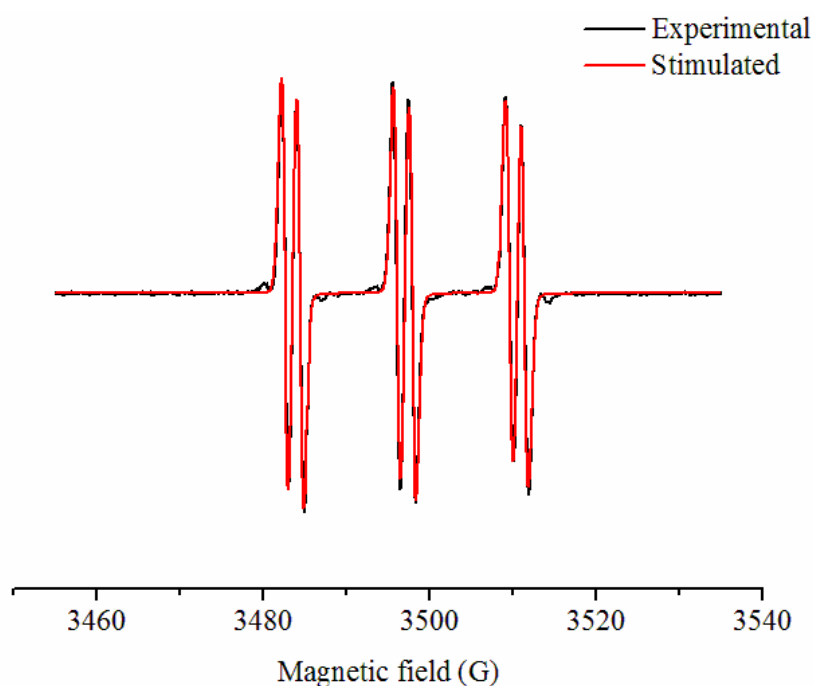


**Figure 6.** ESR spectra of OXE-B under irradiation of LED@405 nm in tert-butylbenzene ( $1 \times 10^{-3}$  mol/L)

The  $\text{CO}_2$  was released during the decarboxylation process where the active radical was generated after 5s irradiation. Specifically, the N-O bond of OXE-B was cleaved upon irradiation of LED@405 nm and the acyloxy radical was produced, 74.2% acetoxy radical ( $\text{CH}_3\text{COO}\cdot$ :  $\alpha_{\text{N}} = 13.5$  G and  $\alpha_{\text{H}} = 1.8$  G) was found in the OXE-B system and was trapped by electron spin resonance (ESR) (See Figure 6). Meanwhile, 25.8% methyl radicals ( $\alpha_{\text{N}} = 14.6$  G and  $\alpha_{\text{H}} = 3.70$  G) were found in ESR [40,41]. which also corresponded to the polymerization efficiency and the detection of  $\text{CO}_2$ .

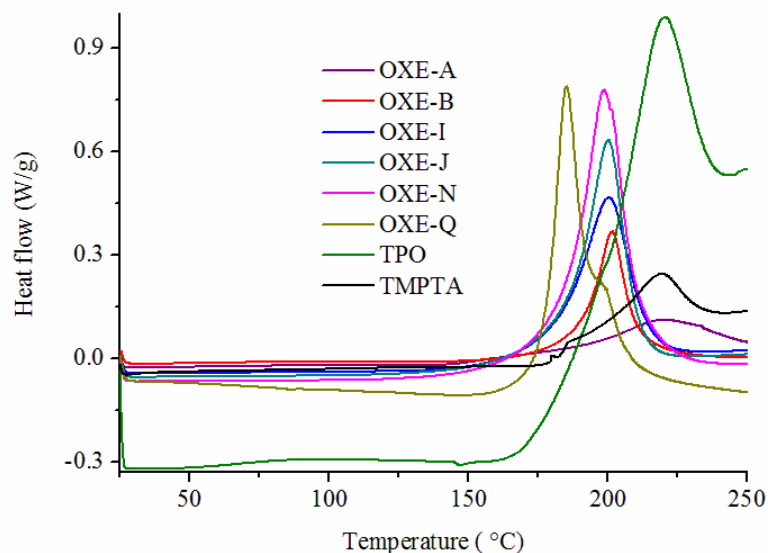
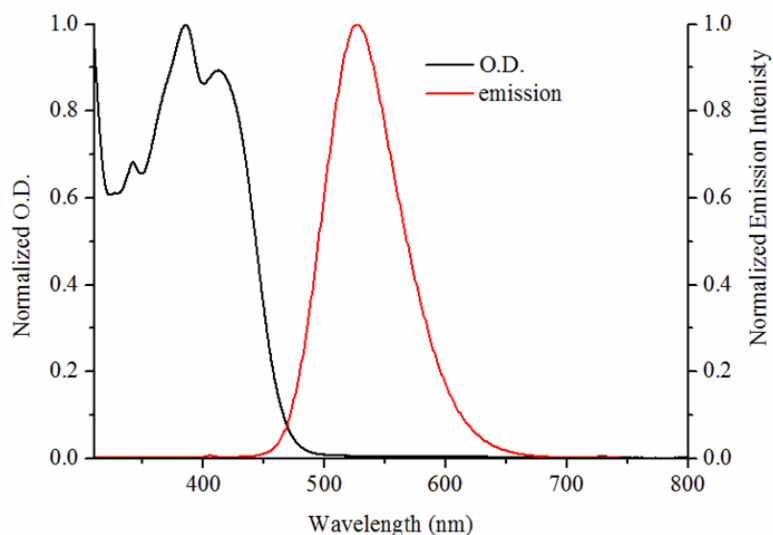


**Table 1.** Some thermal polymerization parameters of OXEs

PIs	T <sub>initial</sub> (°C)	T <sub>max</sub> (°C)	FC (%)
OXE-A	133	220	2.28
OXE-B	141	202	7.97
OXE-I	132	201	8.32
OXE-J	138	202	9.97
OXE-N	126	200	14.84
OXE-Q	145	187	13.7
TPO	175	245	15.95
TMPTA	180	246	2.34

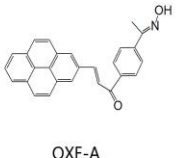
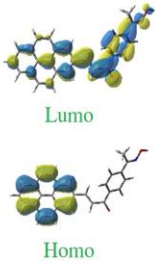
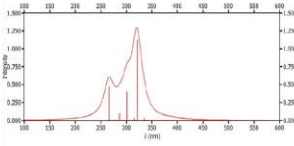
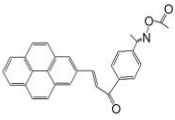
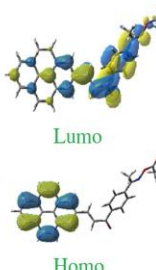
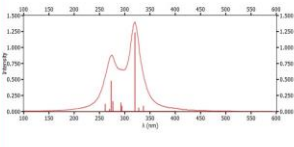
Pyrene-chalcone oxime esters also can generate free radicals through thermal degradation. In order to evaluate these oxime esters' thermal polymerization capability, the differential scanning calorimetry (DSC) experiment was carried out. DSC curves (heat flow vs temperature) of OXE-A, OXE-B, OXE-I, OXE-J, OXE-N, OXE-Q, TPO in TMPTA and pure TMPTA only are presented in Figure 7, and some parameters in Table 1. T<sub>initial</sub> (the temperature when thermal polymerization takes place) and T<sub>max</sub> (the temperature when polymerization rate is maximum) as well as the FC of TMPTA. Except for TPO and TMPTA, the T<sub>initial</sub> of these formulas were all below 150 °C (See Figure 7). As shown in table 1 the TPO has the highest FC

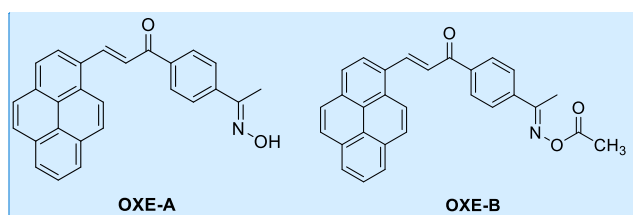
(15.95%), but the  $T_{\text{initial}}$  is higher (175°C), and the TMPTA has a lower FC (2.34%), when the TMPTA paired with OXEs the FC were improved obviously, so these OXEs have the ability of the thermal polymerization.



**Figure 8.** Fluorescence emission and UV-visible spectra of OXE-B ( $1 \times 10^{-4}$  mol/L) in acetonitrile

As shown in Figure 8, the singlet excited-state energy ( $E_{S1}$ ) of OXE-B was caught from the crossing point in the spectra of fluorescence emission and UV-vis absorption, the HOMO and LUMO frontier orbitals and their respective calculated spectrum UV-visible absorption of OXE-A and OXE-B were molecular simulated at the UB3LYP see Figure 9. The  $E_{S1}$  of other OXEs are given in Table 2. The cleavage enthalpies of N-O bond were calculated with  $\Delta H_{\text{cleavage } S1/T1} = \text{BDE}(\text{N-O}) - E_{S1}/E_T$  where BDE is bond dissociation energy, E is the energy of singlet state ( $E_{S1}$ ) or triplet state ( $E_{T1}$ ), which can be used as a reference to judge the favorability of the cleavage [42]. Some relevant parameters are given in Table 2. Except for OXE-A, all the values  $\Delta H_{\text{cleavage } S1} < 0$ , which meant these cleavage enthalpies from  $S_1$  was energetically favorable [43]. Furthermore, cleavage enthalpies from  $T_1$  were also favorable, which meant the cleavage of the N-O bond from  $T_1$  cannot be ignored.

	HOMO/LUMO	$E_T$ (kcal/mol)	BDE (kcal/mol)	Spectrum UV
 OXE-A	 Lumo Homo	49.56	64.57	 (100 nm <math>< 600\text{ nm}</math>) lmax= 373 nm F= 1.127 lmax= 366 nm F= 0.474 lmax= 335 nm F= 0.035 lmax= 300 nm F= 0.012
 OXE-B	 Lumo Homo	48.69	47.35	 (100 nm <math>< 600\text{ nm}</math>) lmax= 320 nm F= 1.238 lmax= 273 nm F= 0.482 lmax= 337 nm F= 0.087 lmax= 401 nm F= 0.012



Structure to be used in order to modify the figure just above

**Commenté [DF3]:** Figures to be used in order to modify the figure jus above.

**Table 2.** The parameters of OXEs calculated by molecular modeling

PIs	N-O BDE (kcal.mol <sup>-1</sup> )	$E_{s1}$ (kcal.mol <sup>-1</sup> )	$\Delta H_{\text{cleavage } s1}$ (kcal.mol <sup>-1</sup> )	$E_T$ (kcal.mol <sup>-1</sup> )	$\Delta H_{\text{cleavage } T1}$ (kcal.mol <sup>-1</sup> )
OXE-A	64.57	61.63	2.94	49.56	15.01
OXE-B	47.35	60.72	-13.37	48.69	-1.34
OXE-C	42.02	60.49	-18.47	48.69	-6.67
OXE-D	41.90	60.72	-18.82	48.69	-6.79
OXE-E	41.45	60.95	-19.5	48.69	-7.24
OXE-F	41.84	60.72	-18.88	48.69	-6.85
OXE-G	41.50	60.26	-18.76	48.69	-7.19
OXE-H	43.82	58.88	-15.06	48.69	-4.87
OXE-I	41.74	61.17	-19.43	48.69	-6.95
OXE-J	46.63	61.17	-14.54	48.69	-2.06

OXE-K	47.29	60.72	-13.43	48.69	-1.4
OXE-L	47.21	60.49	-13.28	48.69	-1.48
OXE-M	47.94	60.26	-12.32	48.69	-0.75
OXE-N	45.91	60.72	-14.81	48.69	-2.78
OXE-O	41.67	60.49	-18.82	48.69	-7.02
OXE-P	45.17	60.72	-15.55	48.69	-3.52
OXE-Q	46.46	60.95	-14.49	48.69	-2.23
OXE-R	44.19	60.95	-16.76	48.69	-4.5

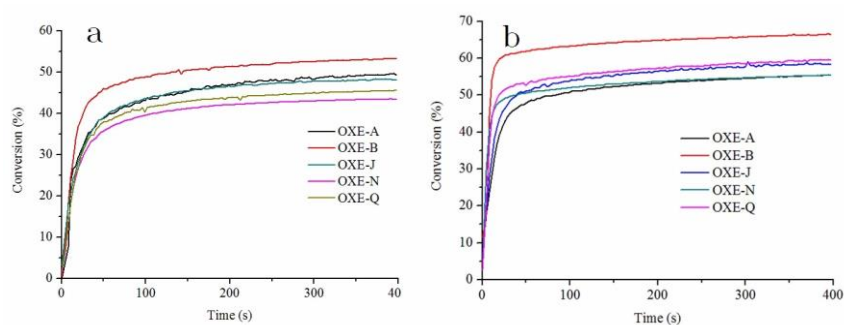
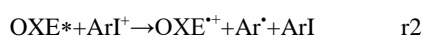


**Figure 10.** Photopolymerization profiles of TMPTA with OXEs-based PIs in laminate (thickness = 25  $\mu\text{m}$ ) upon LED@405 nm starting at  $t = 0$  s, in the presence of (a) OXE-A/OXE-B/OXE-J/OXRE-N/OXE-Q : EDB ( $1 \times 10^{-5}$  mol/g)/( $2 \times 10^{-5}$  mol/g); (b) OXE-A/OXE-B/OXE-J/OXRE-N/OXE-Q : Iod ( $1 \times 10^{-5}$  mol/g)/( $2 \times 10^{-5}$  mol/g)

In order to improve the FC of the TMPTA, EDB and Iod were added into the formulas individually, and the results can be seen in Figure 10. The photopolymerization results showed the OXEs/EDB systems had a higher FC and faster photopolymerization rate than the OXEs without amine (EDB). With the OXEs/EDB ( $1 \times 10^{-5}$  mol/g)/( $2 \times 10^{-5}$  mol/g) used as two-component photoinitiating systems, photopolymerization of TMPTA took place upon the LED@405 nm. The FCs are presented in Figure 10a. The FC trend of these OXEs in thin samples (25  $\mu\text{m}$ , in laminate) is OXE-B > OXE-A > OXE-J > OXE-Q > OXE-N, showing the OXEs/EDB system can improve final function conversions, and faster photopolymerization rates than the OXEs without EDB systems. The OXEs/Iod ( $1 \times 10^{-5}$  mol/g)/( $2 \times 10^{-5}$  mol/g) were used as another two-component systems, and the final function conversions are presented in Figure 10 b. The FC trend of these OXEs

in thin samples (25  $\mu\text{m}$ , in laminate) is OXE-B > OXE-Q > OXE-J > OXE-N > OXE-A, which indicated photopolymerization is not only directly influenced by the absorption properties but also influenced by the interaction between photoinitiator and iodonium salt. The iodonium salt yields electron transfer and generates aryl radicals (illustrated in (r1-r2)).



In order to further understand the role of iodonium salt (Iod) in photopolymerization, oxidation potentials ( $E_{\text{ox}}$ ) were measured by cyclic voltammetry (Table 3), and the result corresponds to the evaluation of the Gibbs free energy ( $\Delta G$ ) of these electron transfer reactions (See Table 3). Remarkably, these strong OXEs/Iod interactions were found in agreement with highly favorable  $\Delta G$ , and the free energy change calculated from  $\Delta G_{\text{S1}} = E_{\text{ox}} - E_{\text{red}}(\text{Iod}) - E_{\text{S1}}$ ;  $E_{\text{red}}(\text{Iod}) = -0.7$  eV.

**Table 3.** Chemical mechanisms parameters of the oxime-esters ( $1 \times 10^{-4}$  mol/L)/Iod ( $2 \times 10^{-4}$  mol/L) system interaction in acetonitrile

PIs	$E_{\text{ox}}$ (eV)	$E_{\text{S1}}$ (eV)	$E_{\text{red}}(\text{Iod})$ (eV)	$\Delta G_{\text{S1}}$ (eV)
OXE-A	1.01	2.69	-0.7	-0.98
OXE-B	1.08	2.65	-0.7	-0.87
OXE-C	1.25	2.64	-0.7	-0.69
OXE-D	1.29	2.65	-0.7	-0.66
OXE-E	1.25	2.66	-0.7	-0.71
OXE-F	1.24	2.65	-0.7	-0.71
OXE-G	1.28	2.63	-0.7	-0.65
OXE-H	1.39	2.57	-0.7	-0.48
OXE-I	1.13	2.67	-0.7	-0.84
OXE-J	1.21	2.67	-0.7	-0.76
OXE-K	1.19	2.65	-0.7	-0.76
OXE-L	1.21	2.64	-0.7	-0.73
OXE-M	1.28	2.63	-0.7	-0.65
OXE-N	1.16	2.65	-0.7	-0.79
OXE-O	1.23	2.64	-0.7	-0.71
OXE-P	1.24	2.65	-0.7	-0.71
OXE-Q	1.18	2.66	-0.7	-0.78
OXE-R	1.29	2.66	-0.7	-0.67

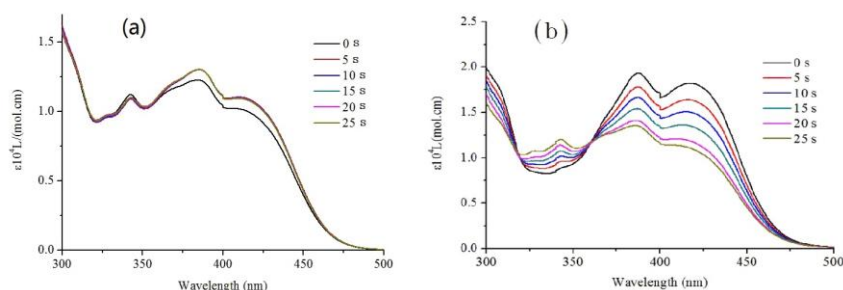


**Figure 11.** (a) Steady-state photolysis of OXE-B ( $1 \times 10^{-4}$  mol/L) and (b) OXE-B ( $1 \times 10^{-4}$  mol/L)/Iod ( $2 \times 10^{-4}$  mol/L) exposed to LED@405 nm in acetonitrile

The steady-state photolysis of OXE-B and OXE-B/Iod in acetonitrile ( $1 \times 10^{-4}$  mol/L) was carried out upon irradiation of LED@405 nm. The photolysis of OXE-B/Iod was faster than the OXE-B without Iod (See Figure 11), indicating a more favorable cleavage of OXE-B/Iod system in the singlet excited state ( $S_1$ ), which fully agrees with the result of the experiment.

It is challenging for photopolymerization to occur inside the black formula, while making carbon fiber composites, using a photoinitiator alone won't yield excellent results. As a dual initiator, OXE-B can be used in this preparation, and demonstrated an excellent performance, the ratio is: (OXE-B ( $1 \times 10^{-5}$  mol/g) Iod ( $2 \times 10^{-5}$  mol/g) / TMPTA/glass fiber (50%/50%, w/w)), the formula was put into transparent polytef mold ( $100 \times 10 \times 2$  mm), first, the formula was irradiated with LED@405 nm up and down individual 10 minutes, then cured in an oven at  $150^\circ\text{C}$  for 10 minutes, last, the carbon fiber composite was stripped from model, the product seen Figure 12 c d. The glass fiber composites ( $100 \times 10 \times 2$  mm) (OXE-B ( $1 \times 10^{-5}$  mol/g) Iod ( $2 \times 10^{-5}$  mol/g) / TMPTA/glass fiber (50%/50%, w/w)) were prepared upon irradiation at 405 nm for 15 minutes (See Figure 12 a,b).

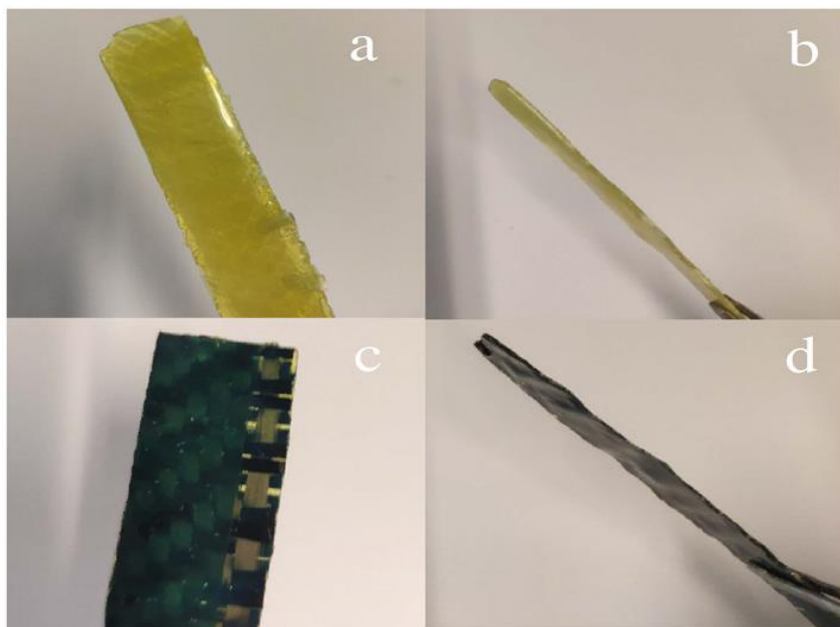


**Figure 12.** (a), (b) glass fiber composites, made of OXE-B ( $1 \times 10^{-5}$  mol/g) and Iod ( $2 \times 10^{-5}$  mol/g) in TMPTA/glass fiber (50%/50%, w/w) and (c),(d) carbon fiber composites made of OXE-B ( $1 \times 10^{-5}$  mol/g) and Iod ( $2 \times 10^{-5}$  mol/g) in TMPTA/carbon fiber (50%/50%, w/w)

Finally, the OXE-B can be used as photoinitiator in 3D laser printing, the OXE-B ( $1 \times 10^{-5}$  mol/g) mixed with monomer TMPTA, the irradiation source was from a laser diode with the intensity of  $110 \text{ mW} \cdot \text{cm}^{-2}$ , the letter pattern “IS2M” for the Institute Science Material Mulhouse was written (See Figure 13), The printed pattern letters has good spatial resolution, and high is about  $1770 \mu\text{m}$ . Obviously, OXE-B will has broad prospects in the 3 D laser print.

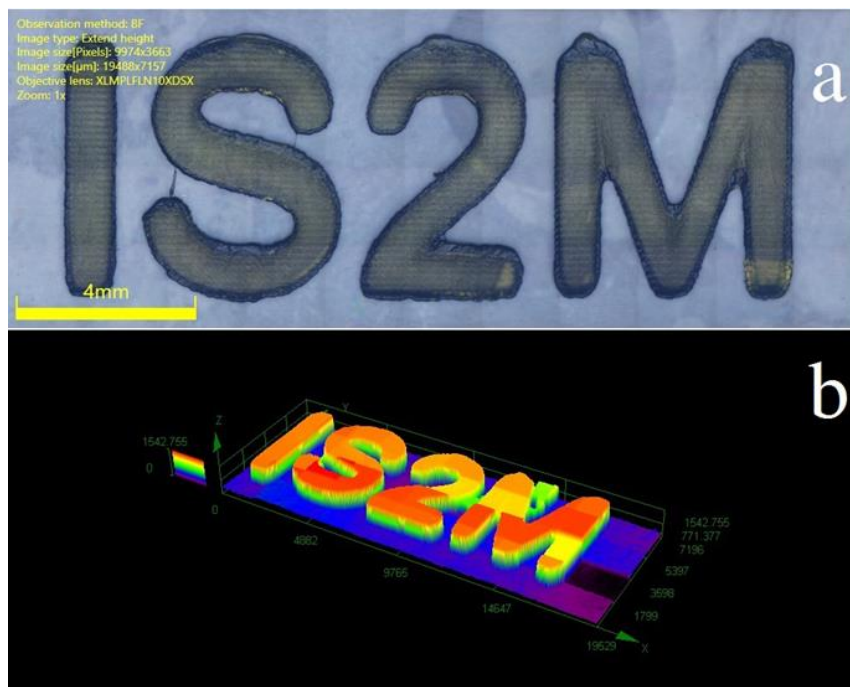


**Figure 13.** Characterization of the letter pattern “IS2M” (a) the view picture, (b) the 3D picture

### Conclusion

In this study, eighteen pyrene-chalcone chromophore-based oxime-esters were successfully synthesized, and seven of these OXEs demonstrated excellent light absorption in the near UV and visible wavelength. Photopolymerizations were evaluated upon the irradiation of a LED@405 nm. OXE-B exhibited a higher final function conversation than others. In order to explain the mechanism of the photopolymerization, some substituent effect/chemical structure relationships were discussed. Based on the simulated calculations, ESR and CO<sub>2</sub> detection experiment, the mechanism of the photopolymerization was confirmed. Furthermore, the thermal polymerization was evaluated by DSC. This study gives a direction for the development of pyrene-chalcone chromophore-based OXEs used as dual-cure systems (thermal/photochemical).

**Acknowledgments:** This research project is supported by The Chinese Scholarship

Council for different PhD grants : CSC N°201902425004 for Xiaoxiang Zhang and CSC N°202108330076 for Zheng Liu. The four first authors equally contributed to this work.

## Reference

- [1] C. Noè, M. Hakkarainen, M. Sangermano, Cationic UV-Curing of Epoxidized Biobased Resins, *Polymers*. 13 (2021) 89. <https://doi.org/10.3390/polym13010089>.
- [2] Y. Yuan, C. Li, R. Zhang, R. Liu, J. Liu, Low volume shrinkage photopolymerization system using hydrogen-bond-based monomers, *Progress in Organic Coatings*. 137 (2019) 105308. <https://doi.org/10.1016/j.porgcoat.2019.105308>.
- [3] I.V. Khudyakov, J.C. Legg, M.B. Purvis, B.J. Overton, Kinetics of Photopolymerization of Acrylates with Functionality of 1–6, *Ind. Eng. Chem. Res.* 38 (1999) 3353–3359. <https://doi.org/10.1021/ie990306i>.
- [4] S.H. Dickens, J.W. Stansbury, K.M. Choi, C.J.E. Floyd, Photopolymerization Kinetics of Methacrylate Dental Resins, *Macromolecules*. 36 (2003) 6043–6053. <https://doi.org/10.1021/ma021675k>.
- [5] T. Dikova, J. Maximov, V. Todorov, G. Georgiev, V. Panov, Optimization of Photopolymerization Process of Dental Composites, *Processes*. 9 (2021) 779. <https://doi.org/10.3390/pr9050779>.
- [6] Maffezzoli, A.D. Pietra, S. Rengo, L. Nicolais, G. Valletta, Photopolymerization of dental composite matrices, *Biomaterials*. 15 (1994) 1221–1228. [https://doi.org/10.1016/0142-9612\(94\)90273-9](https://doi.org/10.1016/0142-9612(94)90273-9).
- [7] H. Zhao, J. Sha, X. Wang, Y. Jiang, T. Chen, T. Wu, X. Chen, H. Ji, Y. Gao, L. Xie, Y. Ma, Spatiotemporal control of polymer brush formation through photoinduced radical polymerization regulated by DMD light modulation, *Lab Chip*. 19 (2019) 2651–2662. <https://doi.org/10.1039/C9LC00419J>.
- [8] W. Xi, H. Peng, A. Aguirre-Soto, C.J. Kloxin, J.W. Stansbury, C.N. Bowman, Spatial and Temporal Control of Thiol-Michael Addition via Photocaged Superbase in Photopatterning and Two-Stage Polymer Networks Formation, *Macromolecules*. 47 (2014) 6159–6165. <https://doi.org/10.1021/ma501366f>.
- [9] F. Jasinski, P.B. Zetterlund, A.M. Braun, A. Chemtob, Photopolymerization in dispersed systems, *Progress in Polymer Science*. 84 (2018) 47–88. <https://doi.org/10.1016/j.progpolymsci.2018.06.006>.
- [10] Y. Yuan, C. Li, R. Zhang, R. Liu, J. Liu, Low volume shrinkage photopolymerization system using hydrogen-bond-based monomers, *Progress in Organic Coatings*. 137 (2019) 105308. <https://doi.org/10.1016/j.porgcoat.2019.105308>.
- [11] Ma, X.; Gu, R.; Yu, L.; Han, W.; Li, J.; Li, X.; Wang, T. Conjugated phenothiazine oxime esters as free radical photoinitiators. *Polym. Chem.* 2017, 8, 6134–6142.

- [12] Liu, S.; Graff, B.; Xiao, P.; Dumur, F.; Lalevée, J. Nitro-Carbazole Based Oxime Esters as Dual Photo/Thermal Initiators for 3D Printing and Composite Preparation. *Macromol. Rapid Commun.* 2021, 42, 2100207.
- [13] Dietliker, K.; Jung, T.; Benkhoff, J.; Kura, H.; Matsumoto, A.; Oka, H.; Hristova, D.; Gescheidt, G.; Rist, G. New Developments in Photoinitiators. *Macromol. Symp.* 2004, 217, 77–98.
- [14] Mallavia, R.; Sastre, R.; Amat-Guerri, F. Photofragmentation and photoisomerization of O-acyl- $\alpha$ -oxo oximes: Quantum yields and mechanism. *J. Photochem. Photobiol., A* 2001, 138, 193–201.
- [15] Abdallah, M.; Hijazi, A.; Graff, B.; Fouassier, J.-P.; Rodeghiero, G.; Gualandi, A.; Dumur, F.; Cozzi, P.G.; Lalevée, J. Coumarin derivatives as versatile photoinitiators for 3D printing, polymerization in water and photocomposite synthesis. *Polym. Chem.* 2019, 10, 872–884.
- [16] Zhou, R.; Pan, H.; Wan, D.; Malval, J.-P.; Jin, M. Bicarbazole-based oxime esters as novel efficient photoinitiators for photopolymerization under UV-Vis LEDs. *J. Polym. Sci.* 2020, 58, 1079–1091.
- [17] Xu, J.; Ma, G.; Wang, K.; Gu, J.; Jiang, S.; Nie, J. Synthesis and photopolymerization kinetics of oxime ester photoinitiators. *J. Appl. Polym. Sci.* 2012, 123, 725–731.
- [18] Li, Z.; Zou, X.; Shi, F.; Liu, R.; Yagci, Y. Highly efficient dandelion-like near-infrared light photoinitiator for free radical and thiol-ene photopolymerizations. *Nat. Commun.* 2019, 10, 3560.
- [19] Dietliker, K.; Hüsler, R.; Birbaum, J. L.; Ilg, S.; Villeneuve, S.; Studer, K.; Jung, T.; Benkhoff, J.; Kura, H.; Matsumoto, A.; Oka, H. Advancements in photoinitiators—Opening up new applications for radiation curing. *Prog. Org. Coat.* 2007, 58, 146–157.
- [20] Dworak, C.; Liska, R. Alternative initiators for bimolecular photoinitiating systems. *J. Polym. Sci., Part A: Polym. Chem.* 2010, 48, 5865–5871.
- [21] Wang, W.; Jin, M.; Pan, H.; Wan, D. Phenylthioether thiophene-based oxime esters as novel photoinitiators for free radical photopolymerization under LED irradiation wavelength exposure. *Prog. Org. Coat.* 2021, 151, 106019.
- [22] Kee, Z.-H.; Hammoud, F.; Hijazi, A.; Graff, B.; Lalevée, J.; Chen Y.-C. Synthesis and free radical photopolymerization of triphenylamine-based oxime ester photoinitiators. *Polym. Chem.* 2021, 12, 1286–1297.
- [23] Ma, X.-Y.; Gu, R.-Q.; Yu, L.-J.; Han, W.-X.; Li, J.; Li, X.-Y.; Wang, T. Conjugated phenothiazine oxime esters as free radical photoinitiators. *Polymer Chemistry*, 2017, 8, 6134–6142.
- [24] Zhou, B.; Xing, C. Diverse Molecular Targets for Chalcones with Varied Bioactivities. *Med. Chem.* 2015, 5, 388–404.
- [25] Batovska, D.-I.; Todorova, I.-T. Trends in utilization of the pharmacological potential of chalcones. *Curr. Clin. Pharmacol.* 2010, 5, 1–29.
- [26] Sahu, N.-K.; Balbhadra, S.-S.; Choudhary, J.; Kohli, D.-V. Exploring pharmacological

- significance of chalcone scaffold: a review. *Curr. Med. Chem.* 2012, 19, 209–225.
- [27] Singh, P.; Anand, A.; Kumar, V. Recent developments in biological activities of chalcones: a mini review. *Eur. J. Med. Chem.* 2014, 85, 758–777.
- [28] Karthikeyan, C.; Moorthy, N.-S.; Ramasamy, S.; Vanam, U.; Manivannan, E.; Karunakaran, D.; Trivedi, P. Advances in chalcones with anticancer activities. *Recent. Pat. Anti-Cancer. Drug. Discovery.* 2015, 10, 97–115.
- [29] Sharma, B.; Agrawal, S.-C.; Gupta, K.-C. Colour reactions of chalcones and their mechanism. *Orient. J. Chem.* 2008, 24, 289–294.
- [30] Chen, H.; Noirbent, G.; Liu, S.; Brunel, D.; Graff, B.; Gignes, D.; Zhang, Y.; Sun, K.; Morlet-Savary, F.; Xiao, P.; Dumur, F.; Laleve'e, J. Bis-chalcone derivatives derived from natural products as near-UV/visible light sensitive photoinitiators for 3D/4D printing. *Mater. Chem. Front.* 2021, 5, 901–916.
- [31] Groenenboom, C. J.; Hageman, H. J.; Oosterhoff, P.; Overeem, T.; Verbeek, J. Photoinitiators and Photoinitiation Part 11. The Photodecomposition of some O-acyl 2-oximinoketones. *J. Photochem. Photobiol., A* 1997, 107, 261–269.
- [32] Chen, S.; Jin, M.; Malval, J.-P.; Fu, J.; Morlet-Savary, F.; Pan, H.; Wan, D. Substituted stilbene-based oxime esters used as highly reactive wavelength-dependent photoinitiators for LED photopolymerization. *Polym. Chem.* 2019, 10, 6609–6621.
- [33] Zhou, R.; Sun, X.; Mhanna, R.; Malval, J.-P.; Jin, M.; Pan, H.; Wan, D.; Morlet-Savary, F.; Chaumeil, H.; Joyeux, C. Wavelength-Dependent, Large-Amplitude Photoinitiating Reactivity within a Carbazole-Coumarin Fused Oxime Esters Series. *ACS Appl. Polym. Mater.* 2020, 2, 2077–2085.
- [34] Hammoud, F.; Lee, Z.-H.; Graff, B.; Hijazi, A.; Laleve'e, J.; Chen, Y.-C. Novel phenylamine-based oxime ester photoinitiators for LED-induced free radical, cationic, and hybrid polymerization. *J. Polym. Sci.* 2021, 59, 1711–1723.
- [35] Amat-guerri, F.; Mallavia, R.; Sastre, R. O-Acyl- $\alpha$ -Oxooximes and Related Compounds. Chemistry, Photochemistry, and Use As Photoinitiators for Radical Polymerizations. *J. Photopolym. Sci. Technol.* 1995, 8, 205–232.
- [36] Li, Z.; Zou, X.; Zhu, G.; Liu, X.; Liu, R. Coumarin-Based Oxime Esters: Photobleachable and Versatile Unimolecular Initiators for Acrylate and Thiol-Based Click Photopolymerization under Visible Light-Emitting Diode Light Irradiation. *ACS Appl. Mater. Interfaces* 2018, 10, 16113–16123.
- [37] Schultz, C. P.; Eysel, H. H.; Mantsch, H. H.; Jackson, M. Carbon Dioxide in Tissues, Cells, and Biological Fluids Detected by FTIR Spectroscopy. *J. Phys. Chem.* 1996, 100, 6845–6848.
- [38] Kumar, J.; D'Souza, S. F. Preparation of PVA membrane for immobilization of GOD for glucose biosensor. *Talanta* 2007, 75, 183–188.

- [39] Glen, A.; Russell; Jerrold, P.; Lokensgard. Application of electron spin resonance spectroscopy to problems of structure and conformation. X. .alpha.-Oxo radicals. *J Am Chem Soc.* 1967, 19, 5059–5060.
- [40] Ding, Y.; Jiang, S.; Gao, Y.; Nie, J.; Du, H.; Sun, F. Photochromic Polymers Based on Fluorophenyl Oxime Ester Photoinitiators as Photoswitchable Molecules. *Macromolecules* 2020, 53, 5701–5710.
- [41] Haire, L. D.; Krygsman, P. H.; Janzen, E. G.; Oehler, U. M. Correlation of radical structure with EPR spin adduct parameters: utility of the proton, carbon-13, and nitrogen-14 hyperfine splitting constants of aminoxyl adducts of PBN-nitronyl-13C for three-parameter scatter plots. *J. Org. Chem.* 1988, 53, 4535–4542.
- [42] Hammoud, F.; Giacoletto, N.; Noirbent, G.; Graff, B.; Hijazi, A.; Nechab, M.; Gimes, D.; Dumur, F.; Lalevéé, J. Substituent effects on the photoinitiation ability of coumarin-based oxime-ester photoinitiators for free radical photopolymerization. *Mater. Chem. Front.* 2021, 5, 8361–8370.
- [43] Qiu, W.; Li, M.; Yang, Y.; Li, Z.; Dietliker, K. Cleavable coumarin-based oxime esters with terminal heterocyclic moieties: photobleachable initiators for deep photocuring under visible LED light irradiation. *Polym. Chem.* 2020, 11, 1356–1363.